The EMBO Journal (2006) 25, 3652–3663 | © 2006 European Molecular Biology Organization | All Rights Reserved 0261-4189/06
www.embojournal.org

THE EMBO JOURNAL

C3G regulates the size of the cerebral cortex neural precursor population

Anne K Voss*, Danielle L Krebs and Tim Thomas*

The Walter and Eliza Hall Institute of Medical Research, Parkville, Victoria, Australia

The mechanisms regulating the size of the cerebral cortex are poorly understood. Here, we demonstrate that the Rap1 guanine nucleotide exchange factor, C3G (Grf2, Rapgef1), controls the size of the cerebral precursor population. Mice lacking C3G show overproliferation of the cortical neuroepithelium. C3G-deficient neuroepithelial cells accumulate nuclear β-catenin and fail to exit the cell cycle *in vivo*. *C3G* mutant neural precursor cells fail to activate Rap1, exhibit activation of Akt/PKB, inhibition of the β-catenin-degrading enzyme, Gsk3β and accumulation of cytosolic and nuclear β-catenin when exposed to growth factors, *in vitro*. Our results show that the size of the cortical neural precursor population is controlled by C3G-mediated inhibition of the Ras signalling pathway.

The EMBO Journal (2006) **25,** 3652–3663. doi:10.1038/sj.emboj.7601234; Published online 20 July 2006
Subject Categories: signal transduction; development
Keywords: C3G; cerebral cortex development; neural precursor proliferation; Rap1; ras signalling

Introduction

Intellectual capacity is tightly correlated with cerebral cortex size relative to body size, both during human evolution and among mammalian species. The increase in cerebral cortex size in higher mammals is predominantly an increase in surface area with relatively little increase in cortical thickness (Rakic, 1995). It has been proposed that an increase in the neural precursor population before and during the first half of neurogenesis during prenatal development underlies the increase in cortical size (Caviness *et al*, 1995; Rakic, 1995).

Understanding the genetic regulation of the size of the cerebral neural precursor population *in vivo* is in its infancy. Clearly molecular pathways must exist, which allow differential growth of specific brain areas by regulating the neural precursor population. Among molecules shown to regulate the size of the cerebral neural precursor population *in vivo* are fibroblast growth factor 2 (FGF2) and β-catenin. FGF2 has been shown to be essential for normal cerebral cortex expansion during development (Raballo *et al*, 2000). Overexpression of degradation-resistant β-catenin leads to an immense expansion of the neuroepithelium (Chenn and Walsh, 2002). However, how these molecules may relate to each other while regulating the neural precursor population is not known.

Growth factor signalling via the Ras pathway regulates many biological processes, including cell division, migration, differentiation and survival. Ras proteins are small GTPases that are activated by guanine exchange before stimulating downstream targets, including the mitogen-activated kinase/extracellular signal-regulated kinase (Erk) and phosphatidylinositol-3 kinase (PI3K) pathways (Mitin *et al*, 2005). Key regulatory elements of Ras signal transduction are guanine nucleotide exchange factors (Mitin *et al*, 2005). C3G (Grf2, Rapgef1) is a guanine nucleotide exchange factor for Ras family members (Tanaka *et al*, 1994). C3G is activated in response to extracellular signals, including epidermal growth factor (EGF), nerve growth factor (NGF) (York *et al*, 1998; Kao *et al*, 2001) and integrin binding (Arai *et al*, 1999; Uemura and Griffin, 1999). C3G stimulates guanine nucleotide exchange predominantly on Rap1 (Ohba *et al*, 2001). Rap1 activation can reinforce or oppose the downstream consequences of Ras activation (reviewed in Stork, 2003). For example, Rap1 activation can lead to the sustained activation of Erk in differentiating pheochromocytoma cells (PC12) (York *et al*, 1998; Kao *et al*, 2001) or inhibition of Erk in proliferating fibroblasts (Schmitt and Stork, 2002). Very little is known about the circumstances under which C3G/Rap1 act as agonists or antagonists of Ras.

In vivo C3G is essential for embryonic development to proceed normally. *C3G* null embryos die around day 5.0 of gestation (Ohba *et al*, 2001) precluding the study of the function of C3G in nervous system development, where C3G is expressed at higher levels than elsewhere in the embryo. However, we previously generated a *C3G* hypomorphic allele, $C3G^{gt}$, which produces less than 5% normal protein allowing survival of the $C3G^{gt/gt}$ mutant embryos up to embryonic day 14 (E14.5) (Voss *et al*, 2003). $C3G^{gt/gt}$ mutant embryos die due to a blood vessel maturation defect (Voss *et al*, 2003). Interestingly, $C3G^{gt/gt}$ mutant embryos display defects in the developing nervous system before the onset of blood vessel maturation. Lack of C3G causes abnormalities in the proliferating neural precursor population and in differentiating neurons. The role of C3G in neural precursors is the subject of this study.

We show here that C3G deficiency leads to an increase in nuclear β-catenin and causes a prominent increase of neural precursor proliferation in the cerebral cortex. Our findings suggest that C3G signalling is required to activate Rap1 in response to extracellular stimuli, restrict Akt/PKB activation, alleviate Gsk3β inhibition, limit cytosolic and nuclear accumulation of β-catenin, and to restrict the size of the cerebral cortex precursor population. We provide a functional link between one novel player, C3G, two downstream effectors,

*Corresponding authors. AK Voss or T Thomas, The Walter and Eliza Hall Institute of Medical Research, Parkville, Victoria 3050, Australia. Tel.: +61 3 9345 2642; Fax: +61 3 9347 0852;
E-mails: avoss@wehi.edu.au or tthomas@wehi.edu.au

Received: 28 October 2005; accepted: 20 June 2006; published online: 20 July 2006

Akt/PKB and Gsk3β, and two known regulators, FGF2 and β-catenin, of the size of the cerebral cortex.

Results

C3G gene expression

The *C3G* gene is expressed in all cells at low levels (Voss *et al*, 2003). Higher levels of *C3G* expression are observed throughout the neural tube at E9.5 and in the cerebrocortical neuroepithelium at E11.5 and E12.5 (Figure 1).

C3G mutant embryos exhibit an overproliferation of the cerebrocortical neuroepithelium

$C3G^{gt/gt}$ embryos exhibit an enlarged cerebrocortical neuroepithelium at E12.5 (Figure 2A versus B). In contrast, the differentiation fields, where postmitotic neurons undergo differentiation, were reduced in size (Figure 2A versus B). Outwardly, $C3G^{gt/gt}$ embryos were of normal size and indistinguishable from littermate controls. $C3G^{gt/gt}$ mutant mice display variable penetrance of phenotypic abnormalities. At E14.5, the cerebral neuroepithelium was either simply expanded (Figure 2C versus D) or organized in folds (Figure 2E versus F) to accommodate the enlarged cerebral tissues in a normal sized head ($n = 6$, 3, and 3 mutants versus 6, 3, and 3 littermate controls at E12.5, E13.5 and E14.5, respectively). The extent and the cell density of the E12.5 cerebrocortical neuroepithelium ventricular zone were assessed on serial sections using the volumetric method of Cavalieri (Coggeshall, 1992) and the optical dissector method (West *et al*, 1991), respectively (Figure 2G–K). The tissue volume of the ventricular proliferation zone per section (Figure 2H) and its cell density (Figure 2I) were highly significantly increased in the $C3G^{gt/gt}$ mutants compared to controls, which combined to an increased total number of cells per hemisphere in $C3G^{gt/gt}$ mutants (Figure 2K; $n = 5$ $C3G^{gt/gt}$ mutant and 5 control embryos). In contrast, the E14.5 differentiation zone overlying the ventricular zone was reduced in size (Figure 2M versus L). Other parts of the developing brain and spinal cord did not show a significant increase in size.

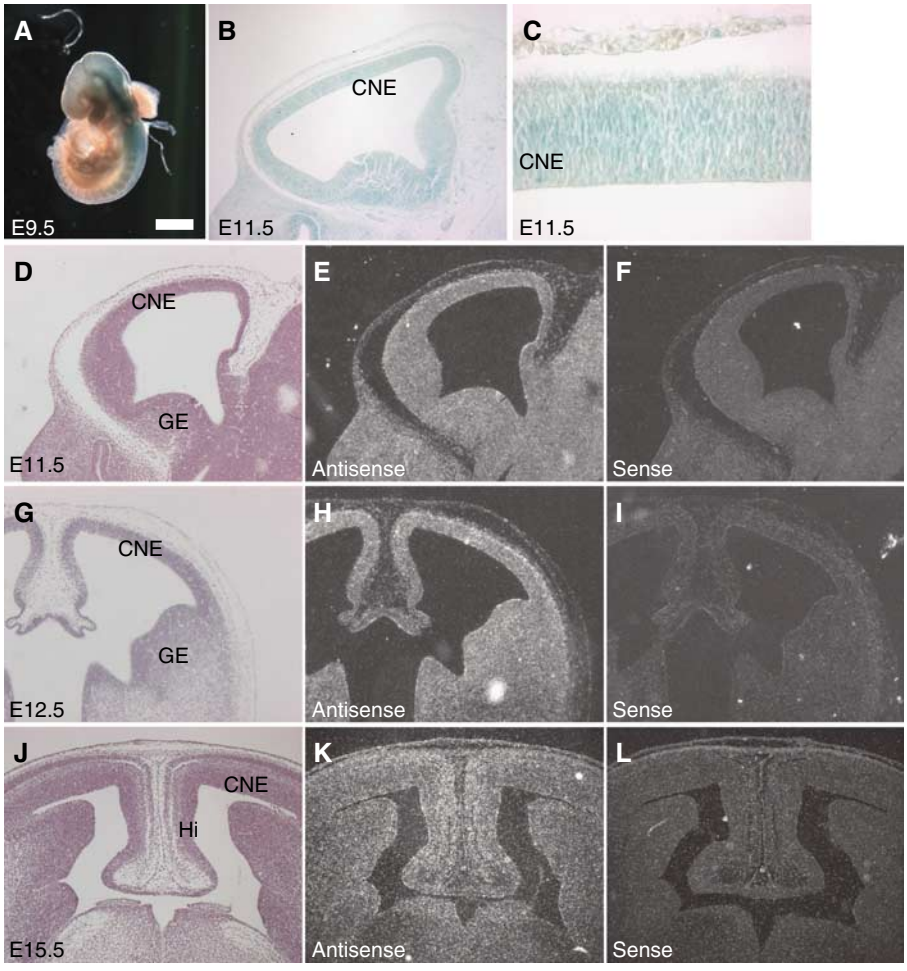

Figure 1 The *C3G* gene is expressed ubiquitously at low levels with higher levels of expression in the developing neuroepithelium. (**A–C**) Histochemical staining (blue) for activity of the β-galactosidase reporter gene inserted in the $C3G^{gt}$ allele (Voss *et al*, 2003). Whole mount E9.5 (A) and sections of E11.5 forebrain (B, C) are shown. (**D–L**) Endogenous *C3G* gene activity was assessed by *in situ* hybridization on paraffin sections of E11.5 (D–F), E12.5 (G–I) and E15.5 (J–L) forebrain using a [^{35}S]-UTP-labelled *C3G* cRNA probe as described (Voss *et al*, 2003). Bright field images are shown in (D, G, J), antisense probe hybridizations in (E, H, K) and sense probe controls in (F, I, L). The location of *C3G* mRNA molecules is revealed by precipitated silver grains, which appear white in the dark field images. Note the low levels of β-galactosidase staining and low density of silver grains, both reflecting the low level of *C3G* gene expression overall with slightly higher levels in the neuroepithelium. CNE, cerebrocortical neuroepithelium; GE, ganglionic eminences; Hi, hippocampal neuroepithelium. Scale bar equals 625 μm in (A), 227 μm in (B, D–I), 28 μm in (C) and 54 μm in (J–L).

An increase in cell number can be caused by three different mechanisms, namely an acceleration of the cell cycle, a failure to exit the cell cycle and a decrease in developmental cell death. We investigated these three options.

Cell death was assessed by TUNEL and corroborated by examining TUNEL-positive cells for chromatin condensation ($n=3$ E11.5 mutants and 3 littermate controls). No difference was observed in the number of TUNEL-positive cells within the neuroepithelial proliferation zone between *C3G* mutant and control brains (data not shown).

To assess the cell cycle length, we determined the fraction of neural precursor cells in S phase as compared to the total proliferating population by incorporation of the thymidine analogue, bromodeoxyuridine (BrdU) at E11.5 and E12.5 ($n=3$ mutants versus 3 littermate controls at each time point). In the developing neuroepithelium, varying lengths of the G_1 phase underlie variations observed in cell cycle length, whereas the length of the S phase is comparably constant (Takahashi *et al*, 1995). Therefore, a change in cell cycle length would lead to a change in the ratio of cells in the S phase over the total proliferating population (BrdU labelling index). Both the total number of cells in the proliferation zone and the number of cells in S phase of the cell cycle within the *C3G* mutant neuroepithelial proliferating zone were significantly elevated (Figure 3A versus B, and C). As both parameters were increased proportionally, the BrdU labelling index was unchanged (Figure 3C), indicating that the relative lengths of S- and G_1-phase were unaltered. We conclude that the length of the cell cycle is not likely to be changed significantly in $C3G^{gt/gt}$ mutants. Other parts of the developing brain and spinal cord showed a tendency towards higher BrdU incorporation. However, the overproliferation of the cerebrocortical neuroepithelium was highly significant, showing that C3G regulates the size of the neural precursor population most prominently in the cortex.

We assessed cell cycle exit by examining BrdU incorporation and staining for the cell cycle marker Ki67 at 0600 on E13.5, 12 h after a single BrdU injection at 1800 on E12.5 ($n=3$ mutants and 3 littermate controls). In this experiment, cells that have left the cell cycle after being exposed to BrdU in their last S-phase will stain strongly for BrdU (green) and weakly for Ki67 (red). Ki67 marks S-, G2-, M- and part of the G1-phase of the cell cycle. However, cells that have only recently exited the cell cycle still contain low levels of Ki67. Cells leaving the cell cycle during this period will also begin to migrate away from the ventricular zone. In contrast, those cells remaining in the cell cycle will undergo further cell division and dilute the BrdU label. These cells will stain weakly for BrdU and strongly for Ki67.

By comparing cell cycle exit in $C3G^{gt/gt}$ mutant (Figure 3E) with wild-type littermate controls (Figure 3D), we saw a substantial difference in the number of cells leaving the cell cycle 12 h after a pulse of BrdU. In the wild-type littermate control cortical neuroepithelium, a large number of brightly green, BrdU-positive cells have already reached the nascent preplate (asterix, Figure 3D). In contrast, in the mutant cortical neuroepithelium, very few BrdU-positive cells have migrated away from the ventricular proliferation zone and almost no preplate (differentiation zone) is visible. Since these cells have only recently left the cell cycle, they still contain some Ki67 immunoreactivity. In contrast, the mutant ventricular zone contains a much higher density of strongly Ki67-positive cells and a larger number of cells with BrdU/Ki67 double positive nuclei, in which the BrdU label has been diluted (insets in Figure 3D and E). These results are shown quantitatively in Figure 3F. We conclude that C3G deficient neural precursors are retained in the cell cycle and are more likely to give rise to further neural precursors as compared to control cells expressing normal levels of C3G. A failure to exit the cell cycle would be expected to affect the size of the differentiating population. Indeed, we observed a significant decrease in the volume of the cerebral differentiation fields in the $C3G^{gt/gt}$ mutants as compared to controls ($16.56 \pm 4.06\,\mu m^3 \times 10^6$ versus $39.58 \pm 6.72\,\mu m^3 \times 10^6$, respectively, $P=0.019$). In contrast to the proliferation zones, the cell density in the $C3G^{gt/gt}$ mutant differentiation zones was not different between mutant and control ($P=0.9163$).

C3G deficiency leads to increased levels of cytosolic β-catenin and accumulation of β-catenin in the nucleus

β-Catenin is a multifunctional protein with largely independent roles in cadherin-mediated cell adhesion and signal transduction (Miller *et al*, 1999). In these two processes, β-catenin is an integral part of adherence junctions at the cell membrane and acts as a transcriptional regulator in the nucleus. As β-catenin has been implicated as a molecule regulating neural precursor proliferation (Chenn and Walsh, 2002), we examined if $C3G^{gt/gt}$ neuroepithelium contained more nuclear β-catenin by immunohistochemistry combined with confocal microscopy (Figure 4; $n=3$ mutants and 3 littermate controls each at E11.5, E12.5 and E14.5). As expected, strong β-catenin immunoreactivity near the cytoplasmic membranes reflecting β-catenin in adherence junction was found in both mutants and controls (Figure 4A–F). As seen in control embryos at E12.5, the fraction of nuclear β-catenin is undetectable or very low (Figure 4A and C). However, $C3G^{gt/gt}$ mutant embryos showed clearly detectable

Figure 2 The cerebrocortical neuroepithelium overproliferates in $C3G^{gt/gt}$ mutant embryos. (**A–F**) Haematoxylin and eosin-stained coronal paraffin sections of littermate wild type (upper panels) and $C3G^{gt/gt}$ mutant embryos (lower panels) at E12.5 (A, B) and E14.5 (C–F). Note the expansion of the cerebral neuroepithelium parallel to the luminal surface (arrows in A–D) and the arrangement of the neuroepithelium in folds in $C3G^{gt/gt}$ embryos at E14.5 in the area of the cortical neuroepithelium (white arrow in F) and the hippocampal neuroepithelium (black arrows in F). In addition, there is a paucity of differentiating cells resulting in small differentiation fields of the ganglionic eminences (B versus A). CNE, cerebrocortical neuroepithelium; ET, epithalamus; GE, ganglionic eminence; Hi, hippocampal neuroepithelium. (**G–K**) Parameters of the cerebrocortical neuroepithelium were assessed quantitatively. Note that, while the rostro-caudal extent (G) is not different between $C3G^{gt/gt}$ mutants and littermate controls, the ventricular proliferation zone is significantly enlarged in $C3G^{gt/gt}$ mutants with respect to all other parameters assessed: (H) average tissue volume per section, $P=0.0009$; (I) cell density, $P<0.0001$; (J) total number of cells per section volume, $P<0.0001$; and (K) total number of cells per dorsal telencephalic hemisphere, $P=0.0081$, $n=5$ E12.5 $C3G^{gt/gt}$ mutant and 5 control embryos. $^{***}P<0.001$, $^{**}P<0.01$. (**L, M**) In contrast to the ventricular proliferation zone (VZ), the overlying differentiation zone was reduced in size in the $C3G^{gt/gt}$ mutants at E14.5 (M versus L). Scale bar equals 245 μm in (A, B) and 192 μm in (C–F), 22 μm in (L, M). Data are expressed as means of two hemispheres of five embryos in each group ± s.e.m. Data were analysed by 2 or 3-factorial analysis of variance (ANOVA) with genotype, experimental animal pair ± rostro-caudal level as the independent factors followed by Fisher's *post hoc* test.

levels of nuclear β-catenin immunoreactivity (Figure 4B, D versus A, C, G). The increase in nuclear β-catenin in the mutant neuroepithelium was seen at E12.5 (Figure 4) and E14.5 (not depicted), the times when the greatest enlargement of the mutant cerebral neuroepithelium was observed. Changes in the subcellular distribution of β-catenin correlated with changes in proliferative activity, as they were not detected in areas of the embryos other than the cortical neuroepithelium. Likewise, there was no difference in the overall levels of β-catenin in *C3G*$^{gt/gt}$ mutant embryos as compared to controls.

To explore the accumulation of β-catenin further, we isolated cerebrocortical neural precursor cells from *C3G*$^{gt/gt}$ and wild-type littermate control embryos, and cultured them

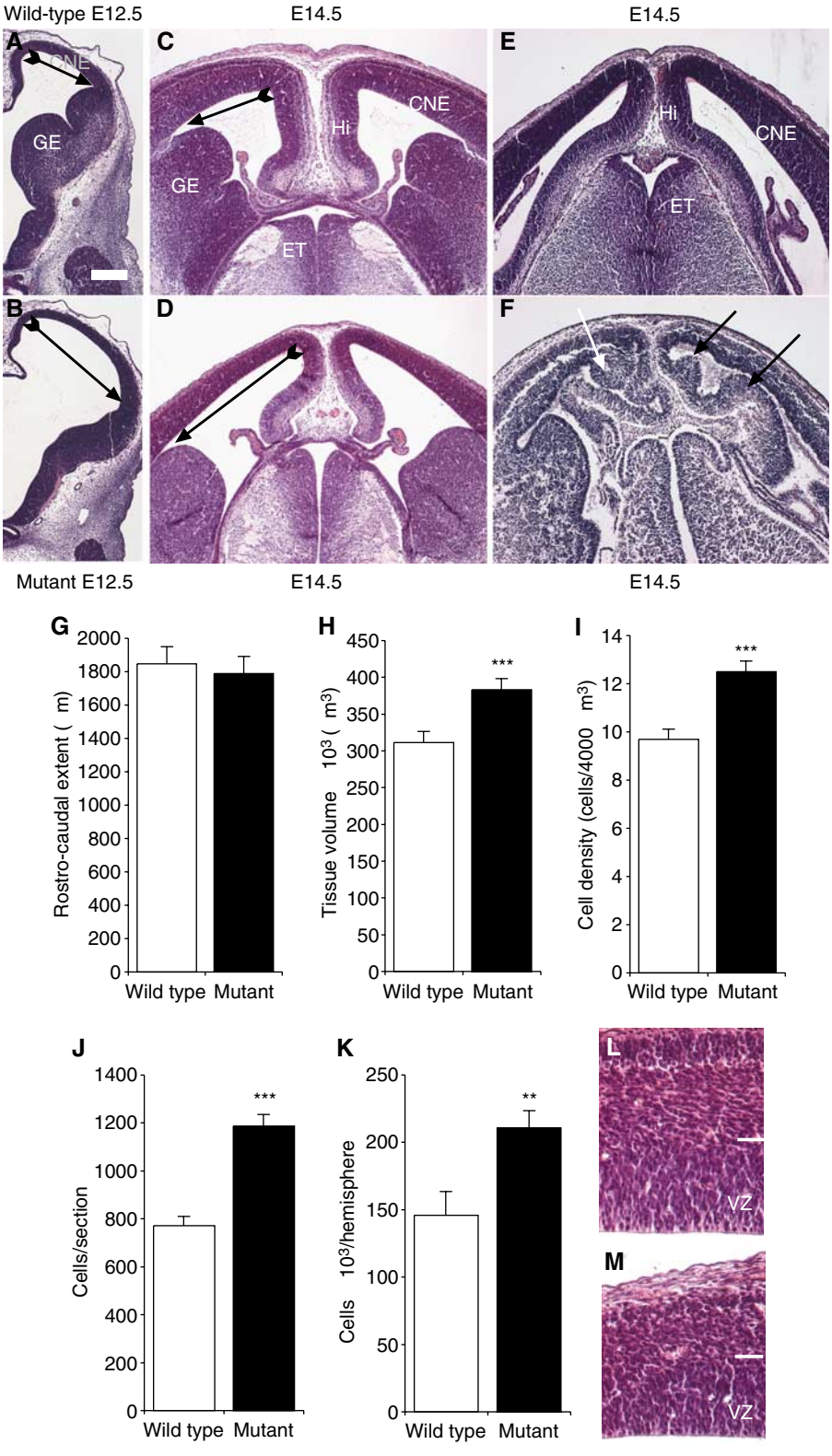

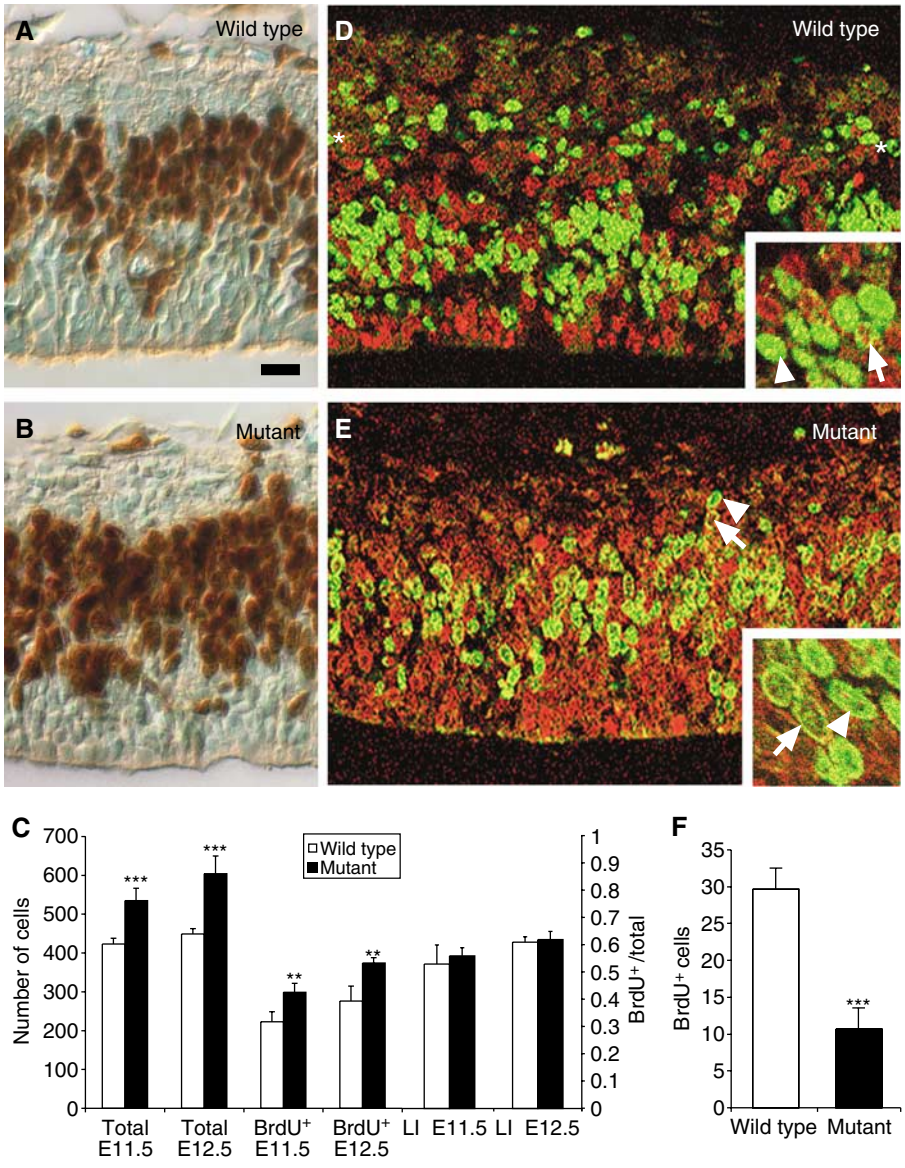

Figure 3 *C3G*$^{gt/gt}$ cerebrocortical neural precursors exit the cell cycle at a reduced rate. (**A, B**) Paraffin sections of E12.5 wild-type littermate (A) and *C3G*$^{gt/gt}$ mutant (B) cerebrocortical neuroepithelium horseradish peroxidase-stained for BrdU (brown). Embryos were recovered 1 h after a single BrdU injection i.p. (100 μg/kg body weight). (**C**) Quantification of the total number of cells (total) and BrdU-positive cells (BrdU$^+$). Cell profiles were counted in the segments of cerebrocortical neuroepithelium above a luminal surface length of 215 μm. Note the increase in both total cell number ($P=0.0005$) and BrdU-positive cells ($P=0.0064$) in the *C3G*$^{gt/gt}$ mutant embryos. The labelling index (LI = BrdU$^+$/total) was not different in the two genotypes. (**D, E**) Confocal images of sections of wild-type littermate (D) and *C3G*$^{gt/gt}$ mutant (E) cerebrocortical neuroepithelium labelled by immunofluorescence for BrdU (green) and the cell cycle marker Ki67 (red). BrdU/Ki67 double positive nuclei are yellow speckled. The embryos were recovered at 0600 on E13.5, 12 h after a single BrdU injection at 1800 on E12.5. Note the presence of strongly BrdU-positive cells in the preplate differentiation zone of the wild-type embryos (asterix in D). Many of these cells are still weakly Ki67-positive. In contrast, *C3G*$^{gt/gt}$ embryos exhibit very few strongly BrdU-positive cells that have migrated away from the ventricular zone, one is indicated with a white arrowhead in (E). Among BrdU/Ki67 double-positive cells, arrows indicate examples with weaker BrdU labelling and arrowheads indicate examples with stronger BrdU labelling (inset in E versus inset in D). (**F**) Quantification of BrdU strongly positive cells. Cell profiles were counted in segments of cerebrocortical neuroepithelium above a luminal surface length of 215 μm. Note the significant reduction in BrdU strongly positive cells, that is, cells that have left the cell cycle since the BrdU injection 12 h earlier, in the *C3G*$^{gt/gt}$ embryos ($P=0.0005$). Data are expressed as means of two hemispheres of three embryos in each group ± s.e.m. Data were analysed by two or three-factorial analysis of variance (ANOVA) with genotype, experimental animal pair ± developmental stage as the independent factors followed by Fisher's *post hoc* test. ***$P<0.001$, **$P<0.01$. Bar = 12 μm in (A, B) and 18 μm in (D, E).

in the presence of FGF2, EGF and insulin *in vitro*. Although the neural precursor cells were cultured in the presence of highly stimulating growth factors, *C3G*$^{gt/gt}$ mutant neural precursor cells still exhibited an increase in nuclear β-catenin immunoreactivity over control cells *in vitro* (Figure 4I and J; mean grey values ± s.e.m. of β-catenin immnuoreactivity assessed on the confocal micrographs were 31.6 ± 1.1 and 69.0 ± 1.1 for wild type and mutant, respectively, $P<0.0001$). Correspondingly, β-catenin levels were increased in the cytosolic fraction of *C3G*$^{gt/gt}$ mutant compared to wild-type neural precursor cells cultured *in vitro* as assessed by Western analysis (Figure 4K) and densitometry (Figure 4M) and also increased in the nuclear fraction, albeit to a lesser extent (Figure 4L and M; results of neural precursor cell cultures

individually isolated from 3 $C3G^{gt/gt}$ mutant and wild-type embryos; $P = 0.0009$; similar results were also observed in a fourth pair of mutant and control cultures). The observed changes in nuclear β-catenin were opposite to, but similar in magnitude to those reported for neurons overexpressing Gsk3β (Lucas *et al*, 2001). As expected, based on the observation by others (Peifer *et al*, 1994; Yost *et al*, 1996; Miller *et al*, 1999) and reported here, the cytosolic and nuclear levels of β-catenin rise concomitantly and the ratio of nuclear to cytosolic β-catenin was not significantly affected by C3G deficiency. As observed *in vivo*, the membrane-associated pool of β-catenin, reflecting β-catenin in adherence junctions, was not affected by C3G deficiency as assessed by cell fractionation and western analysis (data not shown).

We conclude that C3G is required to restrict cytosolic accumulation and hence nuclear localization of β-catenin within the cortical neural precursor population.

Inhibition of Gsk3β promotes proliferation of neural precursor cells in vitro

Nuclear β-catenin was first found to play an integral role as a transcriptional regulator in promotion of proliferation in cancer pathogenesis (Morin *et al*, 1997). Many types of cancer show gain-of-function mutations in the β-*catenin* gene or loss of function in genes coding for proteins forming the β-catenin destruction complex. The β-catenin destruction complex subjects cytosolic β-catenin to proteasomal degradation. Central to the β-catenin destruction complex is glycogen synthase kinase 3β (Gsk3β) (Miller *et al*, 1999). In order to assess if the observed nuclear accumulation of β-catenin could be causally related to an increase in the neural precursor population, we inhibited the β-catenin-degrading enzyme Gsk3β with lithium chloride, which has been shown to lead to accumulation of β-catenin (Klein and Melton, 1996; Stambolic *et al*, 1996). We cultured whole telencephalic hemispheres and cerebral neural precursor cells with and without lithium chloride and assessed DNA synthesis by measuring [^{3}H]thymidine incorporation. We observed that lithium chloride caused an increase in DNA synthesis in telencephalic hemispheres (Figure 5A) and in neural precursor cells (Figure 5B). The effect of lithium chloride was dose-dependent (Figure 5C). The morphology of the cultured neural precursor cell colonies was not altered by the presence of LiCl (Figure 5D versus E). Western analysis of the phosphorylation status of Gsk3β in dorsal telencephalic hemispheres cultured with or without LiCl confirmed increased Ser9 phosphorylation of Gsk3β in the presence of LiCl (Figure 5F), which correlates with Gsk3β inhibition (Cross *et al*, 1995) and an increase in cytosolic and nuclear β-catenin levels assessed by cell fractionation and Western analysis (2.6- and 1.3-fold, respectively, not depicted). This finding is consistent with a causative link between the increase in nuclear β-catenin in $C3G^{gt/gt}$ mutant embryos and the observed expansion of the cerebral neural precursor population.

β-Catenin is a downstream effector of Wnt signalling (Noordermeer *et al*, 1994; Siegfried *et al*, 1994). *Wnt* genes are expressed in the developing cerebral cortex (Grove *et al*, 1998). We examined the expression of *Wnt7a*, *Wnt7b* and *Wnt2b* by RNA *in situ* hybridization. The expression patterns and levels of these *Wnt* genes were not significantly changed in the $C3G^{gt/gt}$ embryos, showing that the patterning of the developing cerebral cortex was not affected by loss of C3G (data not shown).

Lack of C3G leads to an elevated phosphorylation of Erk, Akt/PKB and Gsk3β

C3G is a component of the Ras signalling pathway (Figure 6A). FGF2 and EGF, which are mitogens for neural precursor cells (Drago *et al*, 1991; Reynolds *et al*, 1992; Martens *et al*, 2000), stimulate Ras and Erk activation as well as Ras and Akt/PKB activation (Figure 6A; Kamata and Feramisco, 1984; Whitman and Melton, 1992; Burgering and Coffer, 1995). Akt/PKB activation in turn leads to inhibition of Gsk3β (Cross *et al*, 1995). We utilized mutant and control cells to assess events downstream of C3G signalling.

We analysed activation of Rap1, Erk1/2 and Akt/PKB and inhibition of Gsk3β as downstream events of FGF2 and EGF signalling in $C3G^{gt/gt}$ and wild-type neural precursor cells. Although embryonic neuroepithelial cells do not respond to EGF before E14.5, they acquire EGF-responsiveness within 2 days in culture with FGF2 (Ciccolini, 2001) and so EGF-responsiveness can be studied in proliferating neural precursor cell cultures. After incubation for 4 h without mitogens, we stimulated cells with FGF2, EGF, and/or insulin over a time course of 5 min to 4 h *in vitro* and examined phosphorylation of signal transduction proteins by Western analysis. Wild type and $C3G^{gt/gt}$ mutant cells tolerated 4 h without mitogen and resumed proliferation after mitogens were reapplied. When the cells were stimulated with normal proliferation medium, which contained FGF2, EGF and insulin, we observed a significantly and acutely enhanced phosphorylation of Akt/PKB on Ser473 (Figure 6B and C), corresponding to activation of Akt/PKB (Alessi *et al*, 1996), Gsk3β on Ser9 (Figure 6B and D), corresponding to inactivation of Gsk3β (Cross *et al*, 1995) and Erk1/2 on Thr203/Tyr205 (Figure 6B and E), corresponding to activation of Erk1/2 (Payne *et al*, 1991). Phosphorylation of all three proteins was higher in $C3G^{gt/gt}$ cells as compared to wild-type controls (Figure 6B–E; $n = 3$ mutant and four wild-type cell lines isolated from seven individual embryos). In addition, phosphorylation of Akt/PKB and Gsk3β was prolonged in $C3G^{gt/gt}$ cells (Figure 6C and D).

C3G deficient neural precursor cells respond to FGF2 with enhanced phosphorylation of Akt/PKB and Gsk3β and to EGF with enhanced phosphorylation of Erk

When FGF2, EGF or insulin were used separately to stimulate $C3G^{gt/gt}$ and wild-type neural precursor cells, all three led to increased phosphorylation of Gsk3β, Akt/PKB and Erk1/2 ($n = 6$ mutant and 6 control cell lines isolated from 12 individual embryos). Insulin had similar effects on protein phosphorylation in $C3G^{gt/gt}$ and wild-type cells (data not shown). In contrast, signalling events downstream of FGF2 and EGF were affected by lack of C3G.

FGF2 induced higher Akt and Gsk3β phosphorylation in $C3G^{gt/gt}$ neural precursor cells as compared to control cells (Figure 6F and G), while it induced Erk1/2 phosphorylation (not depicted) to similar levels in both genotypes. In contrast, EGF-induced Erk1/2 phosphorylation was elevated in $C3G^{gt/gt}$ cells (Figure 6H), while EGF-induced phosphorylation of Akt/PKB and Gsk3β (not depicted) was unaffected by C3G deficiency.

An increase in neural precursor proliferation and greater effects downstream of FGF2, namely activation of Akt/PKB and inhibition of Gsk3β, and of the EGF-receptor, namely activation of Erk1/2, in the C3G-deficient cells are consistent with a role of C3G in limiting proliferation in response to FGF2 and EGF. These results suggest that in wild-type neural precursor cells C3G counteracts the phosphorylation (activation) of Akt/PKB and the Ser9-phosphorylation (inhibition) of Gsk3β in response to FGF2, as well as the phosphorylation (activation) of Erk1/2 in response to EGF-receptor activation.

C3G deficiency does not affect basal levels of activated Rap1, but abrogates the ability of cells to respond to external stimuli with Rap1 activation

Rap1 has been reported as the major Ras family target of C3G in fibroblasts (Ohba *et al*, 2001). We assessed the activation status of Rap1 in *C3G*$^{gt/gt}$ mutant and control neural precursor cells. Basal Rap1 activation was not affected by the lack of C3G (Figure 6I), as assessed by RalGDS-GST pull-down of Rap1-GTP from lysates of neural precursor cells incubated for 4 h without mitogens. After stimulation with EGF, FGF2

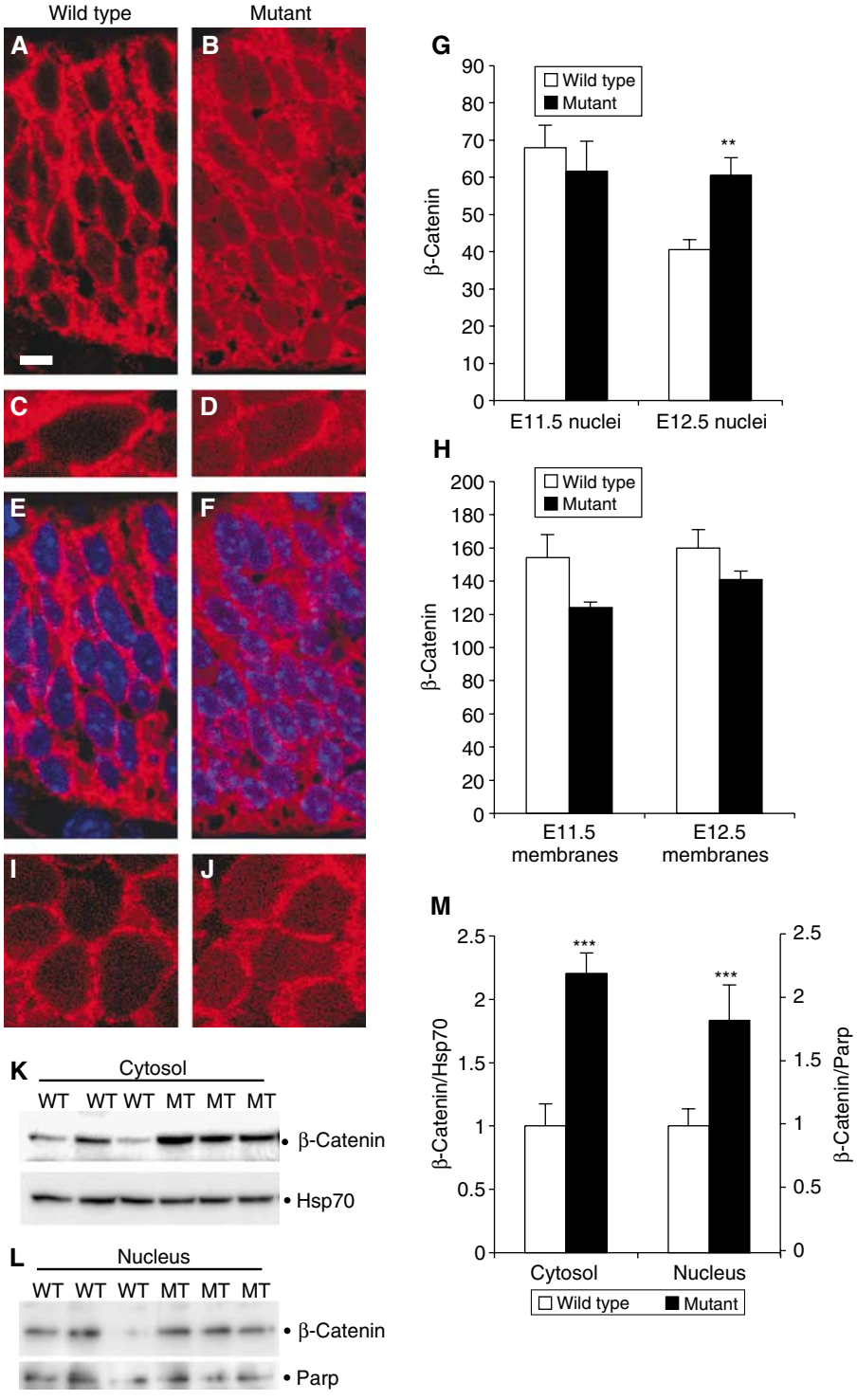

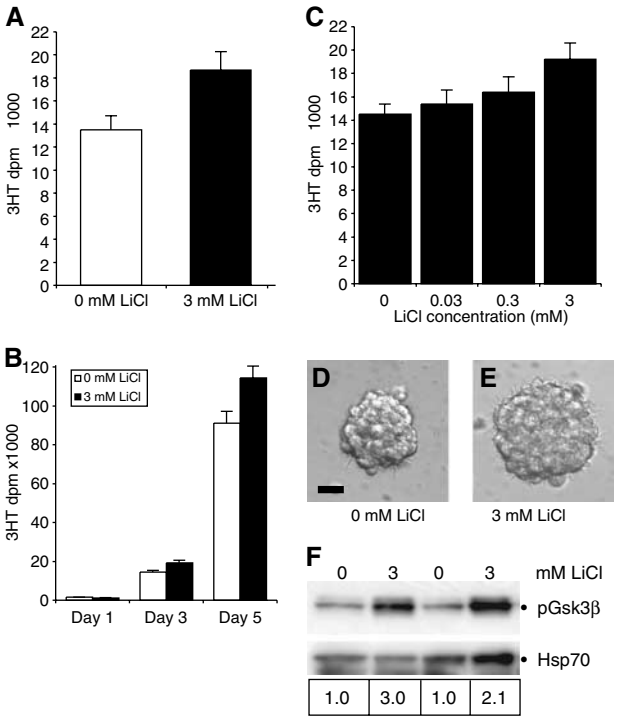

Figure 5 Inhibition of the β-catenin degrading enzyme, Gsk3β, promotes DNA synthesis in cerebrocortical neural precursors. (**A, B**) Quantification of [^{3}H]thymidine incorporation into individual dorsal telencephalic hemispheres (A, $n=20$ dorsal telencephalic hemispheres in each treatment group) or isolated neural precursors cultured as floating colonies (neurospheres) at 5000 cells per 96-well plate well. Addition of lithium chloride (LiCl), an inhibitor of Gsk3β led to an increase in DNA synthesis in all cases ($P=0.0140$ in A and $P<0.001$ in B). (**C**) LiCl-induced increase in DNA synthesis was dose-dependent ($P<0.0001$). (B, C), $n=3$ cell lines isolated from three individual embryos. (**D, E**) Images of neurospheres grown in the presence and absence of LiCl. The morphology of the neurospheres was unaffected by LiCl treatment, except that they grew to a larger diameter compared to controls. (**F**) The effect of LiCl on Gsk3β was assessed by Western analysis of Gsk3β Ser9 phosphorylation, which correlates with Gsk3β inhibition, in dorsal telencephalon hemispheres cultured as in (A). Replicate cultures with 0 or 3 mM LiCl are depicted. Note the prominent increase in Ser9-phosphorylated Gsk3β (pGsk3β) in the presence of LiCl. Hsp70 loading control and densitometry values of pGsk3β relative of Hsp70 are shown below. Data in (A, B) are presented and analysed as stated for Figure 2. The dose–response to LiCl (C) was assessed by regression analysis.

and insulin for 2 min Rap1-GTP was increased in wild type, but not in *C3G*$^{gt/gt}$ mutant cells (Figure 6I). Rap1-GTP was low in mutant and wild-type neural precursor cells after a short exposure to differentiation conditions on laminin without mitogens (Figure 6J). After 3 and 6 days in differentiation conditions, the wild type, but not *C3G*$^{gt/gt}$*mutants* cells showed markedly increased Rap1-GTP (Figure 6J). Ras-GTP loading, as assessed by Raf-1-GST pull-down from total embryo lysates, increased significantly between E10.5 and E12.5 ($P=0.0058$), but was not different between *C3G*$^{gt/gt}$ mutants and controls at E10.5, E11.5 or E12.5 (not depicted). The Rap1 effector B-Raf was present in proliferating neural precursors *in vivo* and *in vitro* as well as in differentiating neural cells *in vitro* (Supplementary Figure 1). The observed requirement of C3G for Rap1 activation in response to stimuli as well as the absence of an effect of C3G deficiency on basal Rap1-GTP levels are consistent with the findings in *C3G* mutant embryonic fibroblasts (Ohba *et al*, 2001).

In conclusion, C3G is required to activate Rap1 in neural cells in response to mitogen stimuli and during differentiation. Furthermore, C3G restricts Erk1/2 and Akt/PKB activation and alleviates Gsk3β inhibition in mitogen-stimulated neural precursor cells. Finally, C3G restricts cytosolic and nuclear accumulation of β-catenin in proliferating neural precursor cells.

Discussion

Molecular consequences of C3G activation

C3G activates predominantly Rap1 (Ohba *et al*, 2001). The downstream molecular effects of C3G-activated Rap1 vary dependent on the cell type, the specific stimulus and other contextual parameters (reviewed in Stork, 2003). Rap1 can inhibit Erk1/2 or PI3K and Akt/PKB activation or, alternatively, induce activation of the same effectors (Stork, 2003). The specific response to Rap1 activation may correlate with cell–substrate interaction. C3G-mediated Rap1 activation correlated with Erk inhibition in CHO cells cultured in suspension, but not in adherent CHO cells (Buensuceso and O'Toole, 2000). In differentiating cell types, Rap1 activation can induce Erk activation, for example, differentiating PC12 cells and megakaryocytes (York *et al*, 1998; Garcia *et al*,

Figure 4 *C3G*$^{gt/gt}$ cerebrocortical neural precursors exhibit elevated levels of nuclear β-catenin *in vivo* and *in vitro*. (**A–F**) Confocal immunofluorescence images of paraffin sections of E12.5 wild-type littermate (A, C, E) and *C3G*$^{gt/gt}$ mutant (B, D, F) cerebrocortical neuroepithelium stained for β-catenin. As expected, prominent β-catenin staining (red) is associated with the cell membranes reflecting the large amounts of β-catenin in adherence junctions. Nuclear β-catenin is visible in the *C3G*$^{gt/gt}$ neuroepithelium, but not in wild-type controls (B, D versus A, C). (E, F) An overlay with the nuclear counterstain bisbenzimide (blue). Note that the mutant nuclei appear more purple indicating double labelling. In proliferating neuroepithelial cells, the cytoplasm is scarce such that only a distinction of the membrane-associated compartment and the nuclei is possible (nuclear counterstain in E completely takes up β-catenin-free in spaces in A). (**G**, **H**) Quantification of β-catenin immunofluorescence in nuclei and membranes. Grey values in nuclear and membrane-associated areas of confocal images of eight cells per animal ($n=3$ animals for each genotype each at E11.5, E12.5) were analysed using NIHimage software. Data are presented and analysed as described for Figure 3. Note that *C3G*$^{gt/gt}$ neuroepithelial cells show significantly higher levels of nuclear β-catenin than controls at E12.5, when the overproliferation is also observed on histological sections ($P=0.001$). In contrast, at E11.5, when the overproliferation is not yet histologically detectable, distribution of β-catenin is unaffected by lack of C3G. At the same time points, levels of β-catenin associated with the membranes, although lower in the mutants, are not significantly different from E12.5 wild-type littermate. (**I**, **J**) Wild type (I) and *C3G*$^{gt/gt}$ mutant (J) cerebrocortical neuroepithelial precursors cultured *in vitro* stained for β-catenin. (**K–M**) Assessment of β-catenin levels by Western analysis (K, L) and densitometry (M) of subcellular fractions of cultured neural precursor cells. Note that cultured *C3G*$^{gt/gt}$ neural precursors, like *C3G*$^{gt/gt}$ cerebrocortical neuroepithelial cells *in vivo*, exhibit increased nuclear β-catenin by immunofluorescence (J versus I). In addition, they show a prominent cytosolic accumulation of β-catenin by Western analysis (K, M) and an increase in nuclear β-catenin by Western analysis (L, M; $n=$neural precursor cell lines isolated from 3 *C3G*$^{gt/gt}$ mutant and 3 wild-type littermate control embryos; $P=0.0009$). Densitometry data are presented as means of the total grey value volume ± s.e.m. of β-catenin normalized for the cytosolic protein Hsp70 in the cytosolic fraction, for the nuclear protein Parp in the nuclear fraction and expressed relative to the mean wild-type control value. Data were analysed by two-factorial ANOVA with genotype and subcellular fraction as the two independent factors. Scale bar = 7 μm in (A, B, E, F), 4 μm in (C, D) and in (I, J). Confocal images were taken at 150 nm optical section thickness. $^{**}P<0.01$, $^{***}P<0.001$.

2001). In contrast, Rap1 activation can lead to inhibition of Ras-effectors such as PI3K, Akt/PKB or Erk in some proliferating cell types, for example, fibroblasts and proliferating B-cells (Schmitt and Stork, 2002; Christian *et al*, 2003). A mechanism put forward for these inhibitory effects of Rap1 on Ras signalling is that Rap1 may bind and sequester Ras effectors (Stork, 2003). Our results suggest that proliferating neural precursor cells fall into the latter category, in which C3G/Rap1 activation results in inhibition of downstream events of growth factor receptor activation.

C3G restricts the response to mitogens

FGF2 promotes neural precursor proliferation and it is required for the cerebral cortex to reach its full size. FGF2 mutant embryos exhibit proliferation deficits specifically in the cerebrocortical neuroepithelium (Raballo *et al*, 2000). Our *in vitro* data suggest that C3G deficiency leads to a deregulation of FGF2-induced proliferation in the early neurogenic phase. EGF-receptors and responsiveness to EGF are found in the forebrain from the mid-neurogenic phase onwards (Martens *et al*, 2000). Ablation of the EGF-receptor

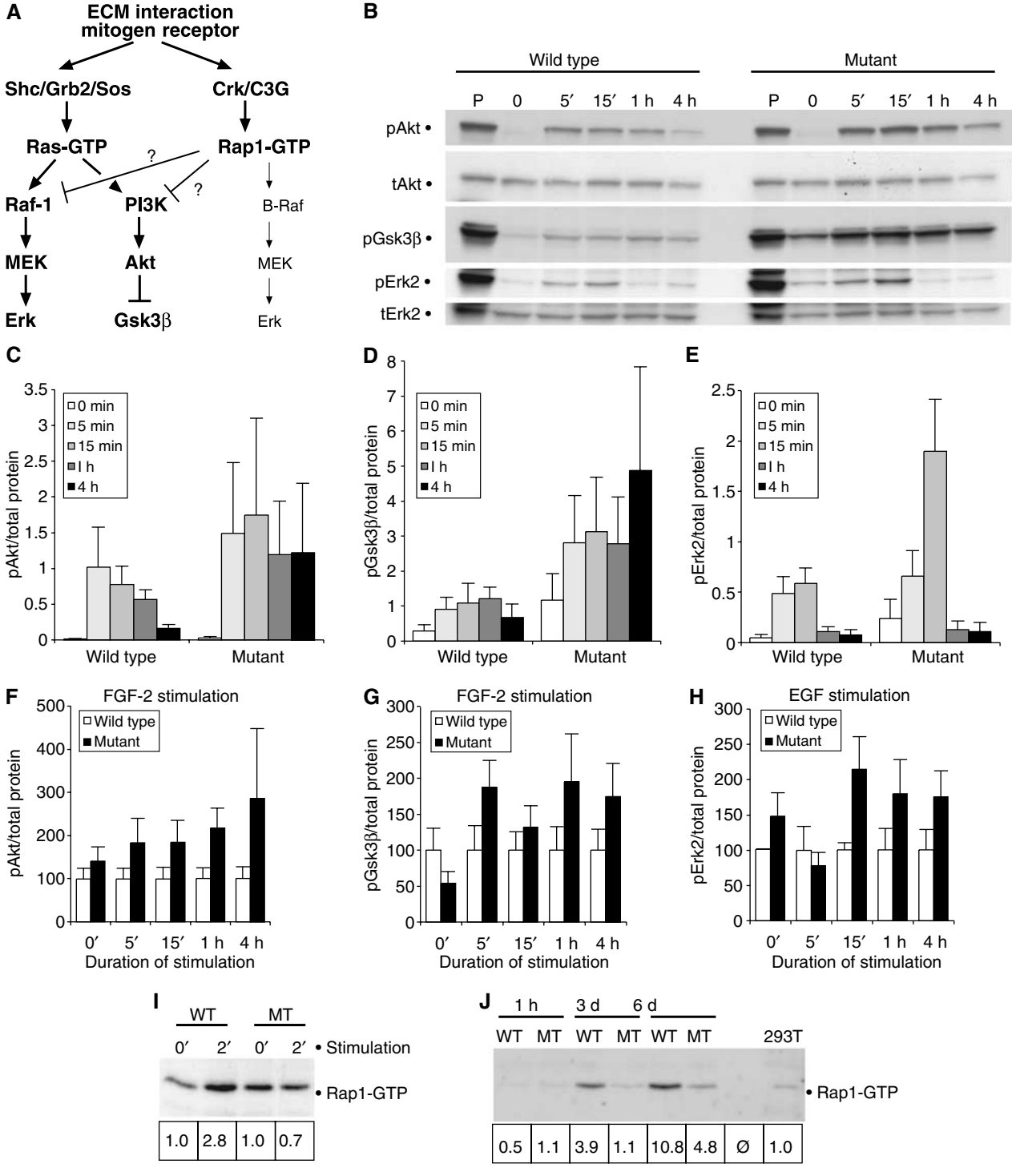

leads to multiple defects including a reduction in brain size (Threadgill *et al*, 1995), while deregulation of EGF-receptor/Ras signalling in the adult brain leads to the formation of tumours (Lassman, 2004), consistent with stimulatory effects of EGF-receptor signalling on brain cell proliferation. During the second half of the neurogenic phase, after the onset of EGF-responsiveness, neural precursor proliferation can be stimulated by both FGF2 and EGF-receptor activation. Our *in vitro* data suggest that C3G deficiency leads to deregulation of both FGF2 and EGF-receptor mediated neural precursor proliferation and result in substantially enhanced overproliferation after EGF-receptor responsiveness has been established. Consistent with the onset of EGF responsiveness between E13.5 and E14.5 (Reynolds *et al*, 1992; Martens *et al*, 2000; Caric *et al*, 2001), we observed extensive overproliferation and fold formation in a subset of the E14.5 $C3G^{gt/gt}$ embryos.

C3G restricts nuclear β-catenin

We report here that *C3G* mutant embryos exhibit an overproliferation of the cerebral neuroepithelium showing that C3G is required *in vivo* to restrict the size of the cerebral cortex during development from E12.5 onwards. That is, the *C3G* mutant phenotype appears at the stage when cells begin to exit the cell cycle and differentiate into neurons. At this time C3G is required to restrict accumulation of β-catenin in the cytosol and hence transfer of β-catenin into the nucleus. β-Catenin is a multifunctional protein with largely independent roles in cadherin-mediated cell adhesion and transcriptional regulation (Miller *et al*, 1999). The majority of β-catenin molecules are localized in adherence junctions at the cell membrane. Free cytosolic β-catenin is subject to Gsk3β-mediated degradation (Miller *et al*, 1999). The transcriptional regulatory function of β-catenin requires stabilization and accumulation of cytosolic β-catenin by inhibition of Gsk3β and so an increase in nuclear β-catenin is associated with an increase in cytosolic β-catenin (Peifer *et al*, 1994; Yost *et al*, 1996; Miller *et al*, 1999; Nelson and Nusse, 2004). The membrane-associated form of β-catenin is neither subject to destruction via cytosolic Gsk3β nor available for its transcriptional regulator function (Nelson and Nusse, 2004). We observed a significant increase in cytosolic and nuclear β-catenin in *C3G* mutant neuroepithelial cells indicating that C3G limits cytosolic and nuclear β-catenin accumulation. Our findings are consistent with the observation that overexpression of degradation-resistant β-catenin induces a massive overproliferation of the cerebral neuroepithelium causing fold formation (Chenn and Walsh, 2002). However, as expected, the *C3G* mutant phenotype is more subtle than the β-catenin overexpression phenotype.

Linking FGF2, C3G, Akt/PKB, β-catenin and proliferation

Our *in vitro* data reveal a mechanism, by which C3G may restrict cerebral neural precursor proliferation and nuclear accumulation of β-catenin, that is, C3G via Rap1 limits FGF2-induced activation of Akt/PKB and thereby limits the inhibition of Gsk3β. Akt/PKB activation has been shown to result in inhibition of Gsk3β (Cross *et al*, 1995). Inhibition of Gsk3β by overexpression of dominant negative Gsk3β leads to nuclear localization of β-catenin (Yost *et al*, 1996). β-Catenin can promote cell proliferation by inducing cyclin D1 promoter activity (Tetsu and McCormick, 1999). Together with these reports, our findings suggest that C3G controls the size of the cortical precursor population by restricting FGF2-induced, Akt/PKB-mediated inhibition of Gsk3β, which would otherwise allow nuclear translocation of β-catenin and enhanced precursor proliferation. C3G provides a negative feedback to proliferation signals exerted on the cerebrocortical neuroepithelium by FGF2.

C3G as a self-limiting mechanism for proliferative signals

Our results indicate a functional interaction between the C3G/Rap1 and the FGF2/Akt/Gsk3β/β-catenin pathway, as well as the EGF/Erk1/2 signalling pathway, providing a mechanism by which the size of the cerebral cortex is specified during development. We propose that growth factors elicit proliferative signals on cerebral neural precursors and concurrently activate a self-limiting mechanism, which clearly requires C3G *in vivo*.

Figure 6 Cell signalling of neural precursor cells in response to extracellular stimuli. (**A**) Schematic diagram of the proposed signalling mechanism involving C3G in proliferating neural precursor cells based on this work. Inhibitory effects of Rap1 on Ras signalling are consistent with our findings in proliferating neural stem cells and have been reported for a number of cell types (reviewed in Stork, 2003). (**B**) Western analysis of phosphorylated Akt (pAkt), Gsk3β (pGsk3β) and Erk2 (pErk2) as well as total Akt (tAkt) and Erk2 (tErk2) of wild-type littermate and $C3G^{gt/gt}$ mutant neural precursor cells stimulated for time durations indicated above with neural stem cell proliferation medium containing 10 ng/ml FGF2, 20 ng/ml EGF and 25 μg/ml insulin after 4 h in basal medium without mitogens. P = proliferation medium prior to experiment, 0 = after 4 h in basal medium without stimulation. (**C**–**E**) Quantification of protein phosphorylation in response to FGF2, EGF and insulin combined. $C3G^{gt/gt}$ mutant cells exhibit higher levels of phosphorylated Gsk3β (D, $P = 0.0046$) and phosphorylated Erk2 (E, $P = 0.0072$) and showed a tendency for higher levels of phosphorylated Akt (C, $P = 0.0693$). (**F**–**H**) Quantification of protein phosphorylation in response to 20 ng/ml FGF2 (F, G) or 20 ng/ml EGF (H) individually. FGF2 stimulated more Akt (F, $P = 0.0021$) and Gsk3β (G, $P = 0.0281$) phosphorylation in $C3G^{gt/gt}$ cells as compared to control cells. EGF stimulated more phosphorylation of Erk2 in $C3G^{gt/gt}$ cells (H, $P = 0.0053$). Densitometry data are presented as means of the total grey value volume ± s.e.m. of phosphorylated protein normalized for total protein or normalized for total protein and expressed as percentage of wild-type control within each experiment and treatment group (B, C, D, $n = 3$ mutant and 4 wild-type neural precursor cell lines isolated from individual embryos; E, F, G, $n = 6$ mutant and six wild-type neural precursor cell lines isolated from individual embryos). Data were analysed by two-factorial ANOVA with duration of stimulation and genotype as the two independent factors followed by Fisher's *post hoc* test. (**I**, **J**) RalGDS pull-down of Rap1-GTP followed by Rap1 Western of total cell lysate of cultured $C3G^{gt/gt}$ mutant (MT) or wild-type (WT) neural precursor cells (I) unstimulated (0′) or stimulated for 2 min (2′) with 10 ng/ml FGF2, 20 ng/ml EGF and 25 μg/ml insulin after 4 h in basal medium without mitogens (input 1 mg protein) or (J) plated onto laminin in the absence of mitogens for 1 h (1 h), 3 days (3 d) or 6 days (6 d; J). Numbers below the bands indicate fold changes over the unstimulated cells (I) or levels compared to 293T cells (J). Note that both $C3G^{gt/gt}$ mutant and control cells exhibit basal Rap1 activation, but only wild-type cells are able to respond to the mitogens with an increase in Rap1-GTP loading (I). Little Rap1-GTP is detectable during the early phase of differentiation (J, 1 h). However, during the course of differentiation, the wild-type cells exhibit higher levels of activation of Rap1 than $C3G^{gt/gt}$ mutant cells (J, 3 d, 6 d).

Materials and methods

Animals, tissue processing, immunodetection, histochemistry, radioactive in situ hybridization and volumetric quantification and cell density assessment

C3G homozygous, heterozygous and wild-type embryos were generated, recovered, genotyped and processed for histology as reported previously (Voss *et al*, 2003). TUNEL, BrdU incorporation studies, immunohistochemistry and immunofluorescence were performed as previously published (Thomas *et al*, 2000; Voss *et al*, 2003). Antibodies used for immunodetection were anti-BrdU (Bio-Science Products, 010198, 1:10), anti-Ki67 (Novocastra NCL-Ki67p, 1:400), anti-β-catenin (BD Transduction, 610153, 1:50). Secondary antibodies used were Vector Laboratories BA-1400, Molecular Probes A-11004, A-11035, A-11029. Whole mount β-galactosidase staining was carried out as previously reported (Voss *et al*, 1998). The volumes of E12.5 cerebrocortical ventricular proliferation zones and differentiation zones were assessed using serial sections using the method of Cavalieri (Coggeshall, 1992) as described previously (Thomas *et al*, 2000). Cell densities were determined by the optical dissector method (West *et al*, 1991) as previously described (Thomas *et al*, 2000).

Cell isolation, culture, lithium chloride stimulation and thymidine incorporation assays

Telencephalic hemispheres with overlying mesoderm and surface ectoderm were dissected under microscopic control from E9.5 and E10.5 embryos from $C3G^{gt/+}$ heterozygous intercrosses. After exposure to pancreatin/trypsin for 30 min at 4°C, the neuroepithelium was pealed away from the overlying mesoderm and surface ectoderm and the dorsal telencephalic neuroepithelium was isolated from the ventral telencephalon as described previously (Thomas and Dziadek, 1993). The dorsal telencephalic neuroepithelium was either cultured whole or dissociated and cultured in neural stem cell proliferation medium as published previously (Rietze *et al*, 2001). Under these culture conditions, neural precursor cells give rise to self-renewing colonies (neurospheres).

For lithium chloride stimulation, dorsal telencephalic hemispheres were cultured in DMEM plus 10% foetal bovine serum for 24 h with or without 3 mM LiCl. Isolated neural precursor cells were cultured in neural stem cell medium as described previously (Rietze *et al*, 2001) with 10 ng/ml FGF2 and 20 ng/ml EGF with concentrations of LiCl as indicated. 5 μCi/ml [^{3}H]thymidine was added 6 h before harvest. DNA was harvested using a 96-well plate cell harvester (Tomtec Harvester 96 Mach IIIM) and [^{3}H]thymidine content was counted using a scintillation microplate counter (Packard TopCount NXT).

Mitogen stimulations and cell lysis

Neural precursor cultures had to be expanded to yield enough material for biochemical studies and so were used for these experiments at passage 5–8. Cultured neurospheres were incubated in serum-free neural stem cell basal medium without mitogens for 4 h and then stimulated with neural stem cell proliferation medium containing 10 ng/ml FGF2, 20 ng/ml EGF and 25 μg/ml insulin or with individual mitogens (20 ng/ml FGF2 or 20 ng/ml EGF or 25 μg/ml insulin), for 2, 5, 15, 60 or 240 min. Cell pellets were washed in phosphate-buffered saline (PBS) and lysed in KALB lysis buffer (150 mM NaCl, 50 mM Tris (pH 7.5), 1% (vol/vol) Triton X-100, 1 mM ETDA, 1 mM Na_3VO_4, 1 mM NaF) containing protease inhibitors (Complete cocktail tablets; Roche). Protein concentrations were determined using the BCA Protein Assay Kit (Pierce) and lysates were used as input for the GTPase activation assays and protein electrophoresis.

Western blotting and GTPase activation assay

Proteins were separated on 4–15% Tris–HCl gels (Bio Rad) and then transferred onto polyvinylidene difluoride membranes (PVDF-Plus, Micron Separations Inc.). Filters were blocked for 1 h in 10% (wt/vol) milk powder in MT-PBS. Primary antibodies were diluted in PBS containing 1% (wt/vol) bovine serum albumin and 0.1% (vol/vol) Tween-20 and were incubated with the filter for 3 h at room temperature. Secondary antibodies were added for 1 h in the same diluent. Blots were stripped by incubation in stripping buffer (1% (wt/vol) SDS, 0.25 M Tris (pH 9.0), 1.92 M glycine, 0.2 M β-mercaptoethanol) for 20 min at room temperature. Western blots were probed for phosphorylated proteins (phospho-p44/42 MAP Kinase (human Thr202/Tyr204 corresponding to murine Thr203/Tyr205) Cell Signaling, #9101; phospho-Akt (Ser 473) Cell Signaling #9271; phospho-Gsk3β (Ser 9) Cell Signaling #9336), then stripped and reprobed for total protein (p44/42 MAP Kinase Cell Signaling #9102; Akt Cell Signaling #9272; Gsk3α/β R&D Systems #AF2157; Hsp70 Calbiochem #386032). Stripping was incomplete for two different antibodies against phospho-Gsk3β (Ser 9). Separate Westerns run to probe only for total protein showed that total Gsk3β and total Akt coincided in relative density in 36 samples (Supplementary Figure 2), such that in subsequent experiments phospho-Gsk3β was normalized to total Akt to avoid quantification on separate blots. Of Erk1 and Erk2 (p44/p42 MAPK), only Erk2 was quantified as it consistently yielded the more prominent band for phosphorylated protein. However, phosphorylation of Erk1 was also induced by the mitogens and appeared to be influenced by C3G-deficiency in a similar manner as Erk2. Western blot signals were quantified using a computing densitometer (Molecular Dynamics). Other antibodies used in Western blots detected Rap1 (Pierce #89872), Ras (Pierce #89855) β-catenin (BD Transduction #610153), B-Raf (Upstate #07–453), Hsp70 (Santa Cruz #sc-24), Parp (Alexis Biochemicals #Alx-804–210), N-cadherin (BD Transduction #610920). To determine Rap1 activation, a GST-RalGDS-Rap1 binding domain affinity purification of Rap1-GTP followed by Rap1 Western analysis was performed according to the supplier's instructions (Pierce #89872). To determine Ras activation, a GST-Raf1-Ras binding domain affinity purification of Ras-GTP followed by Ras Western analysis was performed according to the supplier's instructions (Pierce #89855).

Statistical data analysis

SAS StatView 5.0.1 Software was used to perform multifactorial analyses of variance followed by Fisher's *post hoc* tests or regression analysis as indicated in the figure legends. The default alpha value of the StatView 5.0.1 Software (5%) was used.

Supplementary data

Supplementary data are available at *The EMBO Journal* Online.

Acknowledgements

We are grateful for excellent technical assistance from C Collin, S Mihajlovic, A Morcom and N Ashman. We thank N Nicola, W Alexander and E McManus for fruitful discussions. This work was supported by The Walter and Eliza Hall Institute of Medical Research.

References

Alessi DR, Andjelkovic M, Caudwell B, Cron P, Morrice N, Cohen P, Hemmings BA (1996) Mechanism of activation of protein kinase B by insulin and IGF-1. *EMBO J* **15:** 6541–6551

Arai A, Nosaka Y, Kohsaka H, Miyasaka N, Miura O (1999) CrkL activates integrin-mediated hematopoietic cell adhesion through the guanine nucleotide exchange factor C3G. *Blood* **93:** 3713–3722

Buensuceso CS, O'Toole TE (2000) The association of CRKII with C3G can be regulated by integrins and defines a novel means to regulate the mitogen-activated protein kinases. *J Biol Chem* **275:** 13118–13125

Burgering BM, Coffer PJ (1995) Protein kinase B (c-Akt) in phosphatidylinositol-3-OH kinase signal transduction. *Nature* **376:** 599–602

Caric D, Raphael H, Viti J, Feathers A, Wancio D, Lillien L (2001) EGFRs mediate chemotactic migration in the developing telencephalon. *Development* **128:** 4203–4216

Caviness Jr VS, Takahashi T, Nowakowski RS (1995) Numbers, time and neocortical neuronogenesis: a general developmental and evolutionary model. *Trends Neurosci.* **18:** 379–383

Chenn A, Walsh CA (2002) Regulation of cerebral cortical size by control of cell cycle exit in neural precursors [comment]. *Science.* **297:** 365–369

Christian SL, Lee RL, McLeod SJ, Burgess AE, Li AH, Dang-Lawson M, Lin KB, Gold MR (2003) Activation of the Rap GTPases in B lymphocytes modulates B cell antigen receptor-induced activation of Akt but has no effect on MAPK activation. *J Biol Chem* **278:** 41756–41767

Ciccolini F (2001) Identification of two distinct types of multipotent neural precursors that appear sequentially during CNS development. *Mol Cell Neurosci* **17:** 895–907

Coggeshall RE (1992) A consideration of neural counting methods. *Trends Neurosci* **15:** 9–13

Cross DA, Alessi DR, Cohen P, Andjelkovich M, Hemmings BA (1995) Inhibition of glycogen synthase kinase-3 by insulin mediated by protein kinase B. *Nature* **378:** 785–789

Drago J, Murphy M, Carroll SM, Harvey RP, Bartlett PF (1991) Fibroblast growth factor-mediated proliferation of central nervous system precursors depends on endogenous production of insulin-like growth factor I. *Proc Natl Acad Sci USA* **88:** 2199–2203

Garcia J, de Gunzburg J, Eychene A, Gisselbrecht S, Porteu F (2001) Thrombopoietin-mediated sustained activation of extracellular signal-regulated kinase in UT7-Mpl cells requires both Ras-Raf-1- and Rap1-B-Raf-dependent pathways. *Mol Cell Biol* **21:** 2659–2670

Grove EA, Tole S, Limon J, Yip L, Ragsdale CW (1998) The hem of the embryonic cerebral cortex is defined by the expression of multiple Wnt genes and is compromised in Gli3-deficient mice. *Development* **125:** 2315–2325

Kamata T, Feramisco JR (1984) Epidermal growth factor stimulates guanine nucleotide binding activity and phosphorylation of ras oncogene proteins. *Nature* **310:** 147–150

Kao S, Jaiswal RK, Kolch W, Landreth GE (2001) Identification of the mechanisms regulating the differential activation of the mapk cascade by epidermal growth factor and nerve growth factor in PC12 cells. *J Biol Chem* **276:** 18169–18177

Klein PS, Melton DA (1996) A molecular mechanism for the effect of lithium on development. *Proc Natl Acad Sci USA* **93:** 8455–8459

Lassman AB (2004) Molecular biology of gliomas. *Curr Neurol Neurosci Rep* **4:** 228–233

Lucas JJ, Hernandez F, Gomez-Ramos P, Moran MA, Hen R, Avila J (2001) Decreased nuclear beta-catenin, tau hyperphosphorylation and neurodegeneration in GSK-3beta conditional transgenic mice. *EMBO J* **20:** 27–39

Martens DJ, Tropepe V, van Der Kooy D (2000) Separate proliferation kinetics of fibroblast growth factor-responsive and epidermal growth factor-responsive neural stem cells within the embryonic forebrain germinal zone. *J Neurosci* **20:** 1085–1095

Miller JR, Hocking AM, Brown JD, Moon RT (1999) Mechanism and function of signal transduction by the Wnt/beta-catenin and Wnt/Ca2 + pathways. *Oncogene* **18:** 7860–7872

Mitin N, Rossman KL, Der CJ (2005) Signaling interplay in Ras superfamily function. *Curr Biol* **15:** R563–R574

Moodie SA, Paris MJ, Kolch W, Wolfman A (1994) Association of MEK1 with p21ras. GMPPNP is dependent on B-Raf. *Mol Cell Biol* **14:** 7153–7162

Morin PJ, Sparks AB, Korinek V, Barker N, Clevers H, Vogelstein B, Kinzler KW (1997) Activation of beta-catenin-Tcf signaling in colon cancer by mutations in beta-catenin or APC. *Science* **275:** 1787–1790

Nelson WJ, Nusse R (2004) Convergence of Wnt, beta-catenin, and cadherin pathways. *Science* **303:** 1483–1487

Noordermeer J, Klingensmith J, Perrimon N, Nusse R (1994) dishevelled and armadillo act in the wingless signalling pathway in *Drosophila*. *Nature* **367:** 80–83

Ohba Y, Ikuta K, Ogura A, Matsuda J, Mochizuki N, Nagashima K, Kurokawa K, Mayer BJ, Maki K, Miyazaki J, Matsuda M (2001) Requirement for C3G-dependent Rap1 activation for cell adhesion and embryogenesis. *EMBO J* **20:** 3333–3341

Payne DM, Rossomando AJ, Martino P, Erickson AK, Her JH, Shabanowitz J, Hunt DF, Weber MJ, Sturgill TW (1991) Identification of the regulatory phosphorylation sites in pp42/mitogen-activated protein kinase (MAP kinase). *EMBO J* **10:** 885–892

Peifer M, Sweeton D, Casey M, Wieschaus E (1994) wingless signal and Zeste-white 3 kinase trigger opposing changes in the intracellular distribution of Armadillo. *Development* **120:** 369–380

Raballo R, Rhee J, Lyn-Cook R, Leckman JF, Schwartz ML, Vaccarino FM (2000) Basic fibroblast growth factor (Fgf2) is necessary for cell proliferation and neurogenesis in the developing cerebral cortex. *J Neurosci* **20:** 5012–5023

Rakic P (1995) A small step for the cell, a giant leap for mankind: a hypothesis of neocortical expansion during evolution. *Trends Neurosci.* **18:** 383–388

Reynolds BA, Tetzlaff W, Weiss S (1992) A multipotent EGF-responsive striatal embryonic progenitor cell produces neurons and astrocytes. *J Neurosci* **12:** 4565–4574

Rietze RL, Valcanis H, Brooker GF, Thomas T, Voss AK, Bartlett PF (2001) Purification of a pluripotent neural stem cell from the adult mouse brain. *Nature* **412:** 736–739

Schmitt JM, Stork PJ (2002) PKA phosphorylation of Src mediates cAMP's inhibition of cell growth via Rap1. *Mol Cell* **9:** 85–94

Siegfried E, Wilder EL, Perrimon N (1994) Components of wingless signalling in *Drosophila*. *Nature* **367:** 76–80

Stambolic V, Ruel L, Woodgett JR (1996) Lithium inhibits glycogen synthase kinase-3 activity and mimics wingless signalling in intact cells. *Curr Biol* **6:** 1664–1668

Stork PJ (2003) Does Rap1 deserve a bad Rap? *Trends Biochem Sci* **28:** 267–275

Takahashi T, Nowakowski RS, Caviness Jr VS (1995) The cell cycle of the pseudostratified ventricular epithelium of the embryonic murine cerebral wall. *J Neurosci* **15:** 6046–6057

Tanaka S, Morishita T, Hashimoto Y, Hattori S, Nakamura S, Shibuya M, Matuoka K, Takenawa T, Kurata T, Nagashima K (1994) C3G, a guanine nucleotide-releasing protein expressed ubiquitously, binds to the Src homology 3 domains of CRK and GRB2/ASH proteins. *Proc Natl Acad Sci USA* **91:** 3443–3447

Tetsu O, McCormick F (1999) Beta-catenin regulates expression of cyclin D1 in colon carcinoma cells. *Nature* **398:** 422–426

Thomas T, Dziadek M (1993) Capacity to form choroid plexus-like cells *in vitro* is restricted to specific regions of the mouse neural ectoderm. *Development* **117:** 253–262

Thomas T, Voss AK, Chowdhury K, Gruss P (2000) Querkopf, a MYST family histone acetyltransferase, is required for normal cerebral cortex development. *Development* **127:** 2537–2548

Threadgill DW, Dlugosz AA, Hansen LA, Tennenbaum T, Lichti U, Yee D, LaMantia C, Mourton T, Herrup K, Harris RC, Barnard JA, Yuspa SH, Coffey RJ, Magnuson T (1995) Targeted disruption of mouse EGF receptor: effect of genetic background on mutant phenotype. *Science* **269:** 230–234

Uemura N, Griffin JD (1999) The adapter protein Crkl links Cbl to C3G after integrin ligation and enhances cell migration. *J Biol Chem* **274:** 37525–37532

Voss AK, Gruss P, Thomas T (2003) The guanine nucleotide exchange factor C3G is necessary for the formation of focal adhesions and vascular maturation. *Development* **130:** 355–367

Voss AK, Thomas T, Gruss P (1998) Efficieny assessment of the gene trap aproach. *Dev Dyn* **212:** 171–180

West MJ, Slomianka L, Gundersen HJ (1991) Unbiased stereological estimation of the total number of neurons in the subdivisions of the rat hippocampus using the optical fractionator. *Anat Rec* **231:** 482–497

Whitman M, Melton DA (1992) Involvement of p21ras in *Xenopus* mesoderm induction. *Nature* **357:** 252–254

York RD, Yao H, Dillon T, Ellig CL, Eckert SP, McCleskey EW, Stork PJ (1998) Rap1 mediates sustained MAP kinase activation induced by nerve growth factor. *Nature* **392:** 622–626

Yost C, Torres M, Miller JR, Huang E, Kimelman D, Moon RT (1996) The axis-inducing activity, stability, and subcellular distribution of beta-catenin is regulated in *Xenopus* embryos by glycogen synthase kinase 3. *Genes Dev* **10:** 1443–1454